CHEMISTRY OF MATERIALS

pubs.acs.org/cm Article

Search for Ferroelectric Binary Oxides: Chemical and Structural Space Exploration Guided by Group Theory and Computations

Rohit Batra,[‡] Huan Doan Tran,[‡] Brienne Johnson, Brandon Zoellner, Paul A. Maggard, Jacob L. Jones, George A. Rossetti, Jr., and Rampi Ramprasad*

Cite This: *Chem. Mater.* 2020, 32, 3823−3832 Read Online

ACCESS | Metrics & More | Article Recommendations | Supporting Information

ABSTRACT: The presence of bistable polarization states along with accessible switching capabilities make ferroelectrics an ideal candidate for a variety of applications. Although many conventional ferroelectric (FE) materials, i.e., perovskite-structure-based oxides, have been extensively studied over the past several decades, their success has been limited owing to challenges encountered with scaling down of devices and compatibility with complementary metal−oxide−semiconductor (CMOS) processing. Thus, the surprising discovery of ferroelectricity in thin films (∼30 nm) of hafnia (HfO_2), the first fluorite-structure-type FE material with CMOS compatibility, revived interest in FE memories, among others. However, the most critical lesson to be learned from the example of hafnia is that even binary oxides can be FE if low-lying metastable (or stable) polar phases are present and accessible. In this contribution, we cast a wider net (to go beyond hafnia), involving 20 other simple binary nonmagnetic oxides, in an attempt to systematically reveal (meta)stable polar phases, if any, in such oxides. We employed a combination of structural search methods, first-principles computations, and group-theoretical considerations to find at least five new simple oxides as potential FE candidates—CaO_2 ($Pna2_1$, 33), SrO_2 ($Pna2_1$, 33), Ga_2O_3 ($Pna2_1$, 33), TiO_2 ($Pca2_1$, 29), and Al_2O_3 ($Pna2_1$, 33) with space group information included within parentheses. Among them, the thermodynamic stability and ferroelectric properties of a previously unexplored candidate, CaO_2, was investigated in detail. Structure refinement from synchrotron X-ray diffraction data confirmed that CaO_2 crystallizes in the $Pna2_1$ phase, with structural parameters in agreement with our theoretical predictions. Finally, we provide an assessment of the potential for the practical realization of the identified candidate oxides in their polar phase(s) based our computations presented within the context of the past empirical/theoretical observations and discuss some challenges that still need to be overcome to successfully realize ferroelectricity in simple oxides beyond HfO_2 and ZrO_2. More importantly, this work presents a general strategy to search for ferroelectric or functional materials of any class.

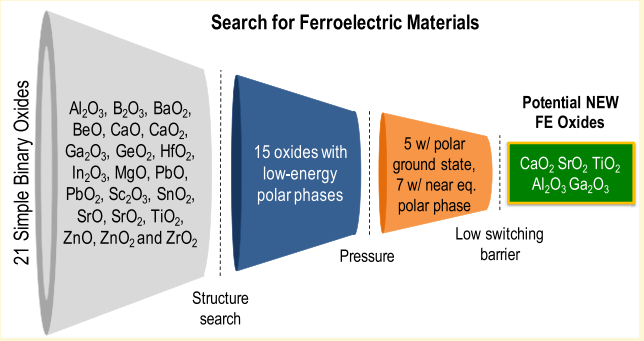

INTRODUCTION

The surprising phenomenon of ferroelectricity discovered in thin films of hafnia[1−5] exemplifies a situation where a novel functionality of a material is unearthed under highly specific conditions.[6−9] In many instances, such unusual material behavior can be traced back to the formation of a new/unknown phase with distinct properties. Likewise, in the case of hafnia, the surprising ferroelectric (FE) behavior has been associated with the formation of the metastable $Pca2_1$ (P−O1) phase owing to poorly understood thermodynamic[10] or kinetic factors.[11] However, from a materials science perspective, an important question that arises from the example of hafnia is how ubiquitous is the phenomenon of ferroelectricity in the class of materials comprising the binary oxides? Is hafnia unique, or are there perhaps many other simple oxides that may show similar FE behavior? While a wide range of perovskite-structured oxides are well known for their superior FE properties, little is known about this phenomenon in binary oxides, with the exception of hafnia and ZrO_2.[5,10] In fact, as a class, binary oxides have been traditionally regarded as linear dielectrics[12−14] owing to limited chemical diversity and the strong covalent nature of the bonds involved.

Nonetheless, an important lesson learned from the example of hafnia is that even binary oxides can display ferroelectricity if low-lying metastable polar phases are present and can be stabilized by intrinsic or extrinsic factors, such as interfaces, strain, doping, electric field, or processing conditions. This

Received: December 23, 2019
Revised: April 10, 2020
Published: April 13, 2020

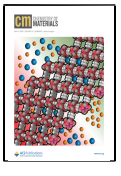

critical realization can be extended to develop a simple and viable strategy to discover new (potential) FE materials. The main elements of such a strategy would entail (1) a meticulous search of the energy landscape of a material of interest to identify many of its low-energy phases, (2) identification of a dynamically stable polar phase with reasonably low energy and high spontaneous polarization value, and (3) if the identified polar phase is not the ground state, an informed search of extrinsic factors which can help to stabilize this material in the identified polar phase. In fact, Huan et al.[15] employed this strategy for the case of hafnia to not only successfully identify the responsible FE P−O1 ($Pca2_1$) phase but also to recommend favorable conditions which may help to realize this metastable FE phase.[7−9]

With the aim of finding superior FE materials or to advance the fundamental scientific understanding of ferroelectricity, several search strategies have been proposed in the past. Such strategies vary in terms of the assumed structure type[16,17] or the involved chemical species,[18] the use of an initial screening step using pre-existing computational/experimental databases,[19,20] or the application of group-theoretical considerations.[21] The present work employs an approach similar to that utilized by Huan et al.[15] but on the members of the class of binary oxides that remain unexplored. A subset of simple binary oxides, i.e., alkaline-earth-metal oxides, has been investigated in the past and was theoretically predicted to display ferroelectricity under large epitaxial strains.[16] This past study, however, assumed the initial structure to be of rock-salt type and exploited the occurrence of imaginary vibrational modes to infer FE behavior and differs from the unconstrained structure search approach adopted here.

Using a combination of theoretical and computational methods, we searched a total of 21 nonmagnetic binary oxide insulators (HfO_2, ZrO_2, TiO_2, SnO_2, CaO_2, SrO_2, ZnO_2, B_2O_3, Sc_2O_3, Al_2O_3, Ga_2O_3, BeO, MgO, CaO, SrO, ZnO, In_2O_3, GeO_2, PbO, PbO_2, and BaO_2), of which many were found to exhibit low-energy metastable polar phases, similar to the case of hafnia. To find cases in which the identified polar phases can become energetically favored or stable, the phase stability of the 15 most interesting oxides was further studied under varying pressures. Five oxides with a polar ground state and seven oxides with a polar phase within 20 meV/atom to the ground state over a pressure range of 0−30 GPa were then studied for their polarization-switching barriers. Overall, five new simple oxides were identified as potential FE candidates, including CaO_2 ($Pna2_1$, 33), SrO_2 ($Pna2_1$, 33), Ga_2O_3 ($Pna2_1$, 33), Al_2O_3 ($Pna2_1$, 33), and TiO_2 ($Pca2_1$, 29), while 2 oxides already known for their potential FE properties (HfO_2 and ZrO_2) were recovered to have low-energy metastable polar phases. Further, our computational study revealed CaO_2 to be the most interesting FE candidate with a polar phase having energy extremely close (within DFT error) to the ground state and a low enough polarization-switching energy barrier. Synchrotron X-ray structure refinement performed on carefully prepared CaO_2 powders confirmed the formation of the polar $Pna2_1$ phase under ambient conditions with measured structural parameters in good agreement with theoretical predictions. Besides proving an assessment of the potential for realization of ferroelectricity (or pyroelectricity) in binary oxides, this work presents a general strategy to search functional (FE, pyroelectric, or polar) materials of any class.

COMPUTATIONAL DETAILS

All theoretical calculations were performed using density functional theory (DFT),[22,23] as implemented in Vienna Ab initio Simulation Package (VASP).[24] We used the kinetic energy cutoff of 500 eV for the plane-wave basis set and the generalized gradient approximation Perdew−Burke−Ernzerhof functional[25] for the exchange-correlation energies. Because the structures examined in this work are significantly different in terms of cell shape, we follow ref 26 to sample the Brillouin zones by a Monkhorst−Pack grid[27] with a spacing of 0.2 $Å^{-1}$ in the reciprocal space.

Identification of the low-energy structures of a given material was the first step of the strategy. This nontrivial task is mathematically formulated as an optimization problem and involves locating the low-lying minima of the potential energy surface (PES) of the material, which is typically constructed from the DFT energy owing to its reliability.[28] Among several modern structure prediction methods, minima hopping[29,30] is a commonly employed powerful method. Starting from a given initial structure, the PES is explored by alternatively applying local optimization and energy barrier crossing steps. While the former is performed with the typical algorithms implemented in regular DFT codes, e.g., VASP, the latter comprises a number of molecular dynamics steps, chosen along the phonon soft-mode directions to improve the efficiency of the method. This method has been successfully used for various classes of materials.[15,31−33]

Standard DFT is formulated at zero temperature (T = 0 K). To access the thermodynamic stability of a given phase at finite temperature T and pressure P, the Gibbs free energy was estimated as $G(T, P) \simeq E_{DFT} + F_{vib}(T) + PV$, where P is the external pressure and V the unit cell volume. In this approximation, the temperature-dependent term, $F_{vib}(T)$, arises from the ionic vibrations of the lattice. Within the lattice dynamic approach, it is given by

$$F_{vib}(T) = 3Nk_BT\int_0^\infty d\omega g(\omega)\ln\left[2\sinh\left(\frac{\hbar\omega}{2k_BT}\right)\right] \quad (1)$$

where k_B is the Boltzmann constant, $\hbar$ is Planck's constant, and N is the number of atoms in the unit cell. The most important input of this expression, e.g., the density of phonon states $g(\omega)$ (ω is the phonon frequency), can be computed within the DFT formalism. The phonon frequencies were computed by evaluating the force constant matrix based on the structures generated using the PHONOPY package[34] and utilizing a supercell with at least a length of 10 Å in each direction. The symmetry of the structures was determined using FINDSYM software.[35] All low-energy structures (both polar and nonpolar) for each of the 21 oxides and other computational files on energy vs pressure behavior, polarization reversal barrier, Born effective charges, etc., that support the findings of this study are available to download at our online repository https://khazana.gatech.edu.

RESULTS AND DISCUSSION

Exploration Strategy. Motivated by the success of the exploration strategy previously used to identify low-energy structures in hafnia (HfO_2),[15] we searched for stable and metastable polar phases of simple oxides. We restricted the space of the search to nonmagnetic and insulating binary oxides. Thus, the list of oxides that were explored consisted of

https://dx.doi.org/10.1021/acs.chemmater.9b05324
Chem. Mater. 2020, 32, 3823−3832

HfO_2, ZrO_2, TiO_2, SnO_2, CaO_2, SrO_2, ZnO_2, B_2O_3, Sc_2O_3, Al_2O_3, Ga_2O_3, BeO, MgO, CaO, SrO, ZnO, In_2O_3, GeO_2, PbO, PbO_2, and BaO_2. We make a note that all of the considered oxides are known to be thermodynamically stable against decomposition, including the alkaline earth metal peroxides CaO_2, SrO_2, and BaO_2.[36,37]

The computation-based search strategy for ferroelectrics, illustrated in Figure 1, involves several steps. First, the

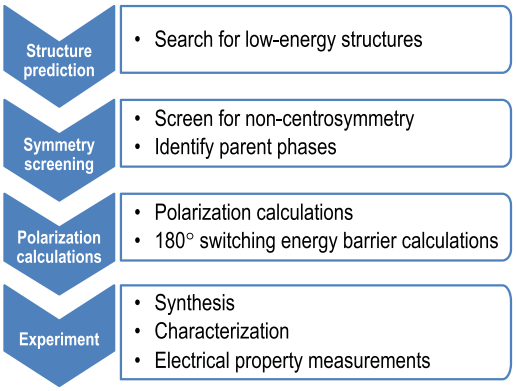

Figure 1. Flowchart illustrating the strategy adopted to find if a particular material is ferroelectric.

structural space of a material was explored, giving a set of low-energy structures. The point group symmetry of these structures was determined to classify them as nonpolar or polar structures. For the latter, the possible parent phase was determined using the group-theoretical considerations enumerated in the classic paper by Shuvalov.[38] The spontaneous polarization of the polar phases was computed via evaluation of the Berry phase,[39,40] while the ease of polarization reversal was evaluated based on the minimum energy pathways determined within the generalized solid-state nudged elastic band (NEB) method.[41] To confirm the spontaneous polarization computations using the Berry phase method, additional polarization calculations using the Born effective charges[42]—evaluated using density functional perturbation theory—and the reference nonpolar phases were also performed. Finally, those oxides with sufficient spontaneous polarization and a low polarization reversal barrier were singled out for further in-depth empirical investigations. Additional computational details on the search of low-energy structures, spontaneous polarization, and reversal pathways are provided in the Computational Details section.

Although the above strategy can be used to determine if a given material is a good FE candidate, it can be computationally demanding when applied to the entire set of 21 oxides considered here. Thus, the following procedure was adopted. First, a structure prediction exploration for all 21 oxides was performed to find the low-energy phases for each. The most interesting oxides, i.e., those which display a low-energy metastable or stable polar phase, were selected next. In all, 15 oxides were found to display either a ground or a metastable polar phase. For these oxides, the influence of an applied external pressure was investigated to determine conditions that may promote or stabilize the identified polar phase(s) in each case. This culminated in the identification of 5 oxides with a stable polar phase and 7 oxides with a polar phase with an energy extremely close (<20 meV/atom) to that of the respective equilibrium phase. Spontaneous polarization and polarization-switching behavior for 11 of these 12 promising oxides were computed next to reveal CaO_2 ($Pna2_1$, 33), SrO_2 ($Pna2_1$, 33), Ga_2O_3 ($Pna2_1$, 33), Al_2O_3 ($Pna2_1$, 33), and TiO_2 ($Pca2_1$, 29) as potential ferroelectrics and Sc_2O_3 ($Cmc2_1$, 36) and B_2O_3 ($Cmc2_1$, 36) as pyroelectrics for the first time. Besides this known ferroelectric (HfO_2[43] and ZrO_2[44]) and pyroelectric (BeO[45] and ZnO[46]) oxides were also recovered. Finally, a detailed study of the most readily accessible FE oxide, i.e., CaO_2, was conducted to estimate its complete phase diagram, which pointed to potential for occurrence of ferroelectricity in CaO_2. To validate this, high-purity CaO_2 powders were synthesized, and structure refinement from synchrotron X-ray diffraction data showed that CaO_2 belongs to space group $Pna2_1$ and is therefore polar. The structural parameters of the polar CaO_2 phase were found to be in perfect agreement with our computations. The overall work flow along with the results obtained at each stage are presented in Figure 2.

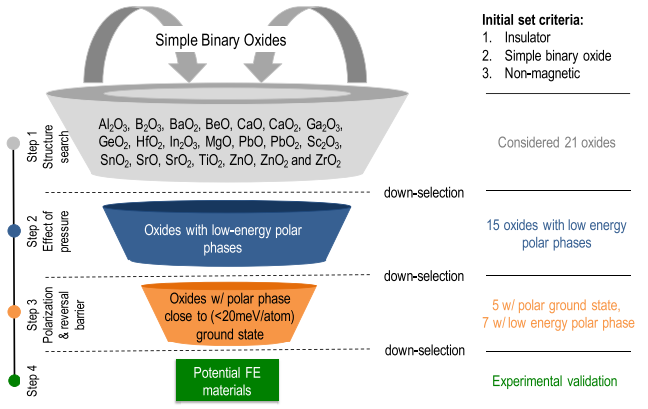

Figure 2. Overall work flow to find potential ferroelectric binary oxides, along with the results obtained in each stage.

Low-Energy Structures. The predicted low-energy structures for all of the oxides are summarized in Figure 3. As described in the Computational Details section, the minima-hopping algorithm along with DFT was used to search for these structures, which were later classified into polar and nonpolar cases based on their point group symmetry. We note that for a few oxides, a low-energy phase crystallizing in space group $P1$ was found. However, we refrain from labeling such cases as polar owing to their low symmetry and availability of only limited empirical evidence supporting the existence of FE materials in space group $P1$.[47] Nonetheless, 15 of the 21 oxides studied can be seen to exhibit low-energy metastable polar states, as highlighted in red in Figure 3. The high occurrence of metastable polar phases in simple oxides clearly indicates that hafnia is not unique among them. Thus, a high probability for discovery of ferroelectricity in other oxides under special conditions—similar to the situation of thin films in the case of hafnia—can be anticipated. To further investigate this possibility, we next studied the subset of 15 promising oxides, which exhibit a low-energy metastable polar phase, to find if pressure can be used to achieve stabilization of a polar phase as the ground state. Nevertheless, our initial search has already revealed interesting oxides with a polar ground state, i.e., BeO and ZnO, and two oxides with polar phase extremely close in energy (within DFT errors) to the ground state in the case of CaO_2 and SrO_2. A detailed

https://dx.doi.org/10.1021/acs.chemmater.9b05324
Chem. Mater. 2020, 32, 3823−3832

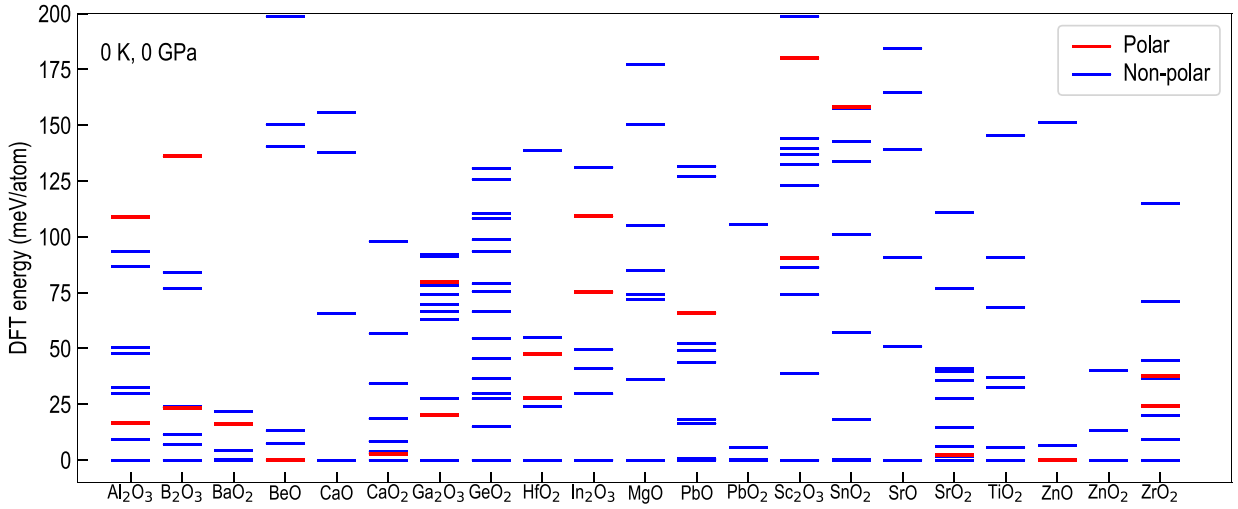

Figure 3. Summary of the low-energy structures obtained from the screening steps. Polar and nonpolar structures are indicated in red and blue, respectively. Only structures within the windows of 200 meV/atom above the lowest energy ground phase are shown (making a polar phase of TiO_2 not visible).

discussion on the polarization magnitude and reversal pathway for these oxides is deferred to later sections. Also, among all of the identified low-energy polar phases in Figure 3, the majority belong to the point group *mm*2, followed by *m* and 2. Further, its not clear what (electronegativity difference, space group, etc.) causes an oxide to display a low-energy polar phase. A detailed analysis of the distribution of polar phases among the different point groups and potential reason for the stability of polar phases is, however, left for future studies.

We make another important note that since the identified phases in Figure 3 were obtained from just a simple structure search (minima-hopping) algorithm, additional phonon computations are necessary to validate their dynamic stability. Owing to the expensive nature of phonon computations, we performed such analysis only for the identified polar phases, which are clearly the most relevant in this work. While most of these polar phases were found to be dynamically stable, there were a few cases which showed imaginary vibrational modes at low pressures, but were found to be dynamically stable at high pressures. Such cases are discussed in detail in the Supporting Information (SI). Thus, all of the polar phases captured in Figure 3 represent a local minima on the potential energy surface, at least within a reasonable range of pressures (0−30 GPa); it should be noted that there is some noise in the DFT phonon computations.[43] Additionally, among the 21 oxides studied, our computations successfully recovered the known ground phase of almost all of the oxides, clearly demonstrating the fidelity of the DFT computations performed in this work.

Effect of Pressure. Figure 4 presents the effect of pressure on the stability of the low-energy polar structures identified earlier. While blue-colored bars represent the difference in the lowest energy polar phase and the equilibrium phase of an oxide at 0 GPa, green-colored bars highlight the *minimum* energy difference between the polar phase and the corresponding ground state of an oxide over a pressure range of 0−30 GPa. Thus, for case where green-colored bars correspond to zero energy difference, i.e., CaO_2, SrO_2, B_2O_3, BeO, and ZnO, the polar phase is indeed the ground state at some pressure value between 0 and 30 GPa; more detailed plots demonstrating the effect of pressure (as well as bandgap) on

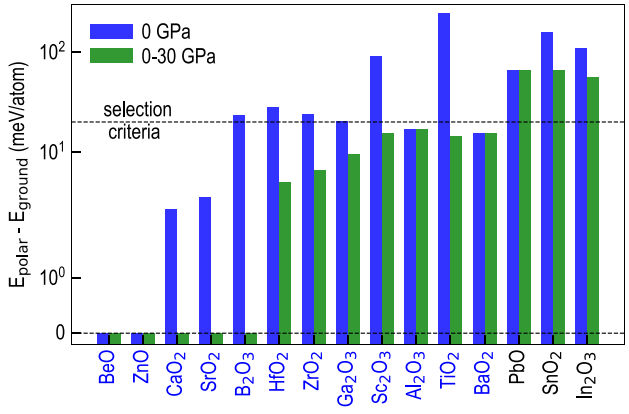

Figure 4. Minimum value of the relative energy of the polar structures at 0 GPa and over the range of 0−30 GPa for the 15 promising oxides. Energies are with respect to the corresponding ground state at a particular pressure.

phase energetics of all 15 oxides are included in the SI. Analogous to the case of hafnia, pressure can be seen to significantly reduce the energy difference between the polar state and the ground state in cases such as ZrO_2, Ga_2O_3, Sc_2O_3, and TiO_2, although it fails to stabilize any polar phase as the thermodynamic ground state. On the other hand, in the case of CaO_2, SrO_2, and B_2O_3, pressure does open up a stability window for the polar $Pna2_1$ (SG 33), $Pna2_1$ (SG 33), and $Cmc2_1$ (SG 36) phases, respectively. Oxides with an energy gap between the polar state and the ground state smaller than 20 meV/atom are highlighted in blue text (cf. Figure 4) and are considered to be promising candidates even though for some cases the polar phase is not the ground state. This is because other extrinsic factors, such as finite size effects, dopants, processing conditions, etc., could be exploited to help stabilize the polar phase in these cases, analogous to the case of HfO_2 where a combination of extrinsic factors has been shown to induce FE behavior through the stabilization of the $Pca2_1$ (SG 29) phase.[7−9] We also note that although we do not perform exclusive computations to find conditions under which the

https://dx.doi.org/10.1021/acs.chemmater.9b05324
Chem. Mater. 2020, 32, 3823−3832

Table 1. Spontaneous Polarization (using Berry phase, Berry, or Born effective charge method, Born) and Polarization Reversal Energy Barriers of Promising Oxides[a]

name	polarization (Berry, $\mu C/cm^2$)	polarization (Born, $\mu C/cm^2$)	NEB barrier (meV/atom)	polar phase	nonpolar phase	potential functionality	new/known
BeO	122	107	120.74	$P6_3mc$	$P6_3/mmc$	Pyro	known
ZnO	82	86	69.42	$P6_3mc$	$P6_3/mmc$	Pyro	known
CaO_2	3.18	3.42	38.54	$Pna2_1$	$P2/c$	FE	new
SrO_2	1.64	1.71	25.53	$Pna2_1$	$P2/c$	FE	new
B_2O_3	79	79	124.38	$Cmc2_1$	$Cmcm$	Pyro	new
HfO_2[43]	52		38	$Pca2_1$	$P4_2/nmc$	FE	known
ZrO_2[44]	58		35	$Pca2_1$	$P4_2/nmc$	FE	known
Ga_2O_3	23	22	16.49	$Pna2_1$	$Pbcn$	FE	new
Sc_2O_3 (20 GPa)	9.4	11.3	92.45	$Cmc2_1$	$Cmcm$	Pyro	new
Al_2O_3	27	27	26	$Pna2_1$	$Pbcn$	FE	new
TiO_2 (30 GPa)	52	57	23.77	$Pca2_1$	$Pbcm$	FE	new
$BaTiO_3$[58]	47		11.2	$P4mm$	$Pm\text{-}3m$	FE	known
$PbTiO_3$[58]	125.5		41	$P4mm$	$Pm\text{-}3m$	FE	known

[a]Details on the space group of the polar and the reference nonpolar phases, expected oxide functionality (Pyro, pyroelectric, or FE, ferroelectric), and if the presented results are new finding are indicated. For comparison, results for two common FEs, $BaTiO_3$ and $PbTiO_3$, are also included.

metstable polar phase can become the ground state, below we include references to past works that report the formation of some of these metastable polar phases under special conditions. The candidates to be considered in the next step include BeO, ZnO, CaO_2, SrO_2, B_2O_3, HfO_2, ZrO_2, Ga_2O_3, Sc_2O_3, Al_2O_3, TiO_2, and BaO_2.

A few noteworthy comparisons between the results obtained in this work can be made with those reported in prior studies. First, the pressure-induced phase transformations obtained from our computations match very well with the past empirical or theoretical studies. For example, the observed transformations from corundum ($R\bar{3}c$) → Rh_2O_3-type ($Pbca$) → $Pbcn$ phase in Al_2O_3,[48] from phase B_2O_3-I ($P3_12_1$ or $P3_1$) → B_2O_3-II ($Cmc2_1$) in B_2O_3,[49,50] from β-Ga_2O_3 ($C2/m$) → α-Ga_2O_3 ($R\bar{3}c$) in Ga_2O_3,[51] from α-PbO ($P4/nmm$) → β-PbO ($Pbcm$) in PbO,[52] and other such pressure-induced phase transformations in the remaining oxides are consistent with our calculations. Second, some of the polar phases identified in this work have been reported in the past. The polar ϵ-Ga_2O_3 ($Pna2_1$) phase has been experimentally observed by heating δ-Ga_2O_3 above 500 °C.[51] Similarly, the polar κ-Al_2O_3 ($Pna2_1$) phase has been observed during chemical vapor deposition (CVD).[53,54] The $Cmc2_1$ is a known high-pressure phase of B_2O_3.[49,50] In the case of TiO_2, the polar $Pca2_1$ phase is believed to form above ∼45 GPa, although the evidence for this is not conclusive.[55,56] The $Pna2_1$ phase is theoretically predicted to have energy extremely close ($\lesssim$2 meV/atom) to the ground state in CaO_2 with an energy difference varying slightly based on the underlying DFT functional.[36] However, in all studies the $Pna2_1$ phase has been found to best fit the experimental XRD data.[36,57] The presence of a polar $Pca2_1$ phase in thin films of HfO_2, ZrO_2, or their solid solutions is well studied in the literature. Thus, there are a number of experimental reports on the formation of polar phases in Al_2O_3, Ga_2O_3, B_2O_3, and TiO_2 that not only further validate our computations but also suggest that existing diffraction data on all of the 15 candidate FE oxides—with low-energy metastable polar phases—should be carefully (re)analyzed to find clues on the formation of the polar phases identified in this work.

Polarization Reversal Barriers and Assessment of Promising Oxides. Besides having a polar ground state, a FE candidate should have a low polarization-switching energy barrier. Thus, for the remaining promising oxides, the computed spontaneous polarization using both the Berry phase and the Born effective charge methods and the polarization reversal energy barriers calculated using the NEB method are presented in Table 1. Space group details of the underlying polar and the reference nonpolar phases are also included. We note that results for HfO_2 and ZrO_2 are obtained from previous works.[43,44] Further, results for Sc_2O_3 and TiO_2 correspond to situations at 20 and 30 GPa pressure, respectively, since the polar phase was found to be closest in energy to the ground state at these pressures. In addition, TiO_2 polar phase was dynamically stable at 30 GPa but not at 0 GPa (see SI). BaO_2 was excluded from this analysis owing to the complex structure of the polar Pm (SG 6) phase.

Considering a well-known FE, such as $PbTiO_3$, has a polarization reversal energy barrier of 41 meV/atom,[58] we can expect CaO_2, SrO_2, Al_2O_3, Ga_2O_3, TiO_2, HfO_2, and ZrO_2 with respective energy barriers of 38.54, 25.53, 26, 16.49, 23.77, 38, and 35 meV/atom to be able to show polarization switching upon application of a sufficient electric field. On the basis of this criteria, we not only successfully recover known FE binary oxides, i.e., HfO_2 and ZrO_2, but also, more importantly, find five new potential FE binary oxides, CaO_2 ($Pna2_1$, 33), SrO_2 ($Pna2_1$, 33), Ga_2O_3 ($Pna2_1$, 33), Al_2O_3 ($Pna2_1$, 33), and TiO_2 ($Pca2_1$, 29), that should be verified experimentally. In contrast, Sc_2O_3, B_2O_3, and BeO were found to have high polarization reversal energy barriers of 92.45, 124.38, and 120.74 meV/atom, respectively, and are expected to be pyroelectric. In fact, BeO is a well-known pyroelectric material,[45] although there have been some contrasting observations of FE loops in BeO as well.[59] Similarly, ZnO with a moderately large polarization reversal energy barrier of 69.42 meV/atom has mostly been reported as a pyroelectric material,[46] with only a few contrasting studies suggesting it to be FE.[60] Overall, our NEB calculations correctly indicate BeO and ZnO as pyroelectric oxides, in agreement with the literature. Subsequently, we predict B_2O_3 ($Cmc2_1$, 36) and Sc_2O_3 ($Cmc2_1$, 36) as potential pyroelectric candidates. We note that for more information on the functionality of these pyroelectric oxides, the pyroelectric coefficient should be calculated, which can be achieved using standard DFT computations. More detailed plots illustrating the polarization

https://dx.doi.org/10.1021/acs.chemmater.9b05324
Chem. Mater. 2020, 32, 3823−3832

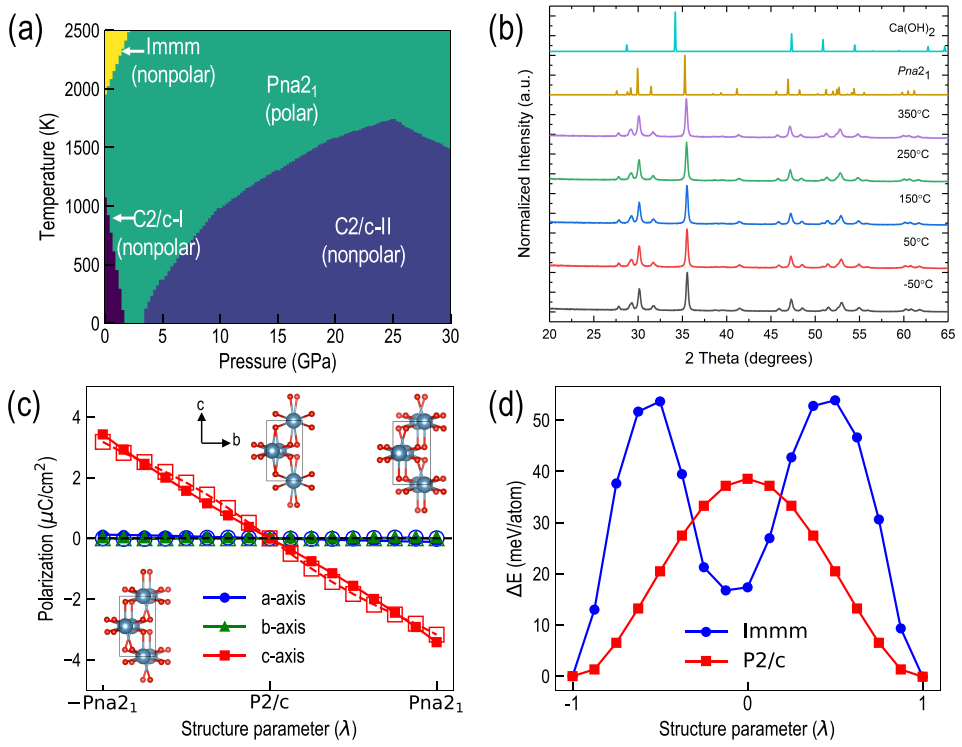

Figure 5. Theoretical and experimental studies to search for potential ferroelectric behavior in CaO_2. (a) Computed phase diagram demonstrating the wide region of stability of the polar *Pna*2$_1$ (SG 33) phase. (b) XRD measurements of CaO_2 powders at different temperatures, confirming the presence of the predicted polar phase. (c) Computed spontaneous polarization of the *Pna*2$_1$ (SG 33) phase using the Born effective charge (solid symbols) and the Berry phase methods (open symbols). (d) Two minimum energy pathways to reverse the polarization as determined using the NEB method.

reversal pathways and the associated polar and nonpolar structures of these candidate oxides are included in SI. From the polarization reversal computations, the associated polarization vs electric field behavior can also be derived assuming the double-well potential approximation.[61] Such analysis could help us estimate coercive fields (E_c), although they could be 1−2 orders of magnitude different from the experimentally measured values, presumably because of other important factors, e.g., the domain wall dynamics and thermal fluctuations (see section E in the SI).

Next, we assess the aforementioned computational results for all 15 candidate oxides with a metastable polar phase and put them in the context of the past literature to determine those that can be most easily be accessed experimentally. The criteria for such an assessment include (i) the polar phase should be the predicted ground state (preferably over a large pressure range), (ii) the computed polarization-switching barrier should be small, (iii) the number of energetically competing nonpolar phases should be small, (iv) preferably there exist some prior empirical reports on the formation of the predicted polar phase, and last, (v) the conditions for stabilization of the predicted polar phase should not be extreme.

Following remarks regarding the potential for the occurrence of ferroelectricity in these oxides can be made. With a polar *Pna*2$_1$ (SG 33) phase extremely close in energy to the ground state, a decent spontaneous polarization, and a low polarization reversal barrier, CaO_2 is likely to be the most easily accessed experimentally as compared to other oxides that require other extrinsic factors to stabilize the polar phase. Further, there have been reports highlighting the possibility of formation of its polar phase.[36] SrO_2 could potentially exist in the polar *Pna*2$_1$ (SG 33) phase, although its computed spontaneous polarization is lower than CaO_2 and has many energetically competing nonpolar phases. Both Al_2O_3 and Ga_2O_3 are promising candidates because of previous reports on formation of κ-Al_2O_3[53,54] and ϵ-Ga_2O_3[51] phases (*Pna*2$_1$, 33), the presence of just two energetically competing nonpolar phases, and the potential stabilization of the polar *Pna*2$_1$ phase under tension (see figures corresponding to the effect of pressure for Al_2O_3 and Ga_2O_3 in the SI). Interestingly, there are reports on the ferroelectricity in Ga_2O_3 films; however, they are for a different polar phase with symmetry *P*6$_3$*mc* (SG 186). TiO_2 is also a potential candidate because of some past studies (though inconclusive) on the stabilization of a polar *Pca*2$_1$ (SG 29) phase at very high pressures of ∼45 GPa.[55,56] PbO has a modest energy difference between the polar and the equilibrium phase, but we do not expect it to be FE as it is unclear under what conditions the polar phase can become stable. We categorize In_2O_3 and SnO_2 as unfavorable cases because of the presence of a large number of other energetically competing phases and because the polar phase has a significantly higher energy than the ground state.

On the other hand, B_2O_3 is identified as a promising pyroelectric candidate (owing to high polarization reversal barrier) for which the polar *Cmc*2$_1$ (SG 36) phase is well known to form under high pressure,[49,50] although no electrical measurements have been made on this phase thus far. With a modest energy difference between the polar and the equilibrium phase, Sc_2O_3 could be potentially pyroelectric, but it is unclear under what conditions the polar phase can become stable.

https://dx.doi.org/10.1021/acs.chemmater.9b05324
Chem. Mater. 2020, 32, 3823−3832

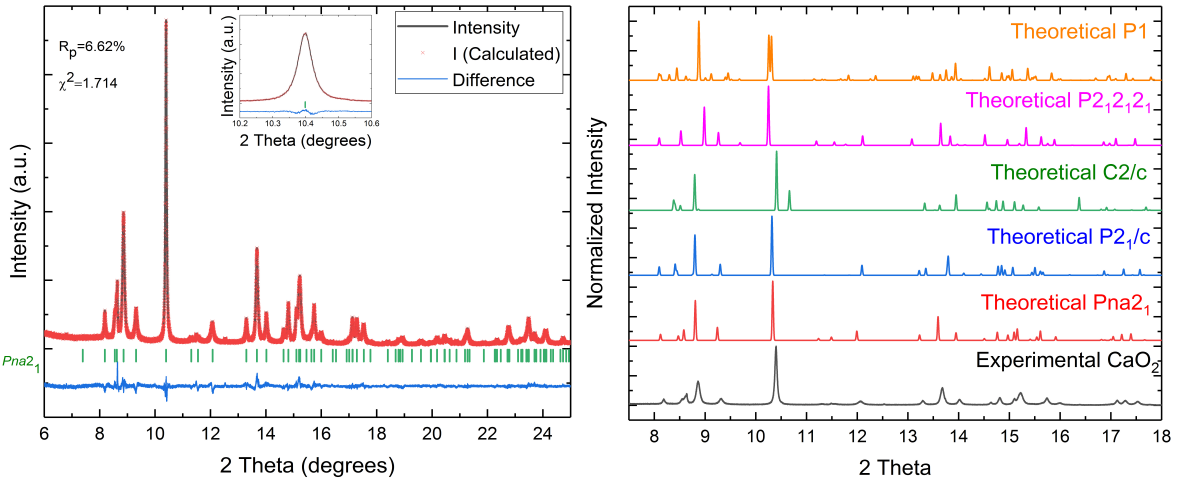

Figure 6. Rietveld refinement and XRD measurements of CaO_2 powders in the $Pna2_1$ (SG 33) phase.

On the basis of a similar assessment, HfO_2 and ZrO_2, which are known for their FE behavior, would have been identified as promising candidates due to a small energy difference between the polar $Pca2_1$ (SG 29) and the equilibrium monoclinic ($P2_1/c$, 14) phase and a small enough polarization reversal barrier. Similarly, BeO and ZnO would have been identified as pyroelectric owing to the high polarization reversal barrier. Overall, both of these cases validate the procedure adopted in this work.

CaO_2 was predicted to have a polar $Pna2_1$ (SG 33) phase extremely close in energy to the ground state $C2/c$-I (SG 15) and is considered next for more detailed investigation. The other low-energy phases found using the minima-hopping approach include $I4/mmm$ (SG 139), $Immm$ (SG 71), $Pmmn$ (SG 59), $P2_12_12_1$ (SG 19), another $C2/c$-II (SG 15), $P2_1/c$ (SG 14), $C2/m$ (SG 12), and $P1$ (SG 1) in the order of decreasing symmetry. However, later, the $I4/mmm$ phase was found to be dynamically unstable as revealed by the imaginary vibrational modes present in its phonon band structure. Thus, using the group-theoretical considerations established by Shuvalov,[38] the centrosymmetric phases $Immm$ and $Pmmn$ with point group symmetry mmm emerge as the plausible parent phase of the polar $Pna2_1$ phase with point group symmetry $mm2$. Shuvalov's study is based on the assumption that the structure of any FE phase can be described by small distortions to a parent prototype phase. Thus, starting from a high-symmetry parent phase, he was able to map all possible FE transitions along with their respective distortions (or symmetry loss). This study can, therefore, be used to identify plausible parent or prototype phase of a known FE based on group-theoretical considerations alone. Furthermore, if one accounts for the energy of these phases, the lower energy $Immm$ can be postulated as the parent prototypical phase of the polar $Pna2_1$ phase of CaO_2.

Using DFT and first-principles thermodynamics, we next computed the free energy of several CaO_2 phases at various pressures and temperatures, as shown in Figure S3 in the SI. From this the CaO_2 phase diagram was created (see Figure 5a), which clearly shows a wide temperature−pressure region where the polar $Pna2_1$ phase is stable. Even at 0 GPa and low temperatures, the ground state $C2/c$-I phase is only ∼2 meV/atom lower in energy than the polar phase, which is within the expected noise of the DFT computations. We note that while the ordering of stability of all of the relevant phases of CaO_2 matches with a previous computational study,[36] the region of stability of the polar $Pna2_1$ phase was found to be substantially larger in this work. One potential source of this discrepancy is the use of different pseudopotentials for the DFT computations. At 0 GPa, the polar $Pna2_1$ (SG 33) phase is predicted to transform to a nonpolar $Immm$ phase around 1800 K, which is in agreement with the group-theoretical considerations discussed above. However, as described below, CaO_2 was found to decompose into $Ca(OH)_2$ above 300 °C in the presence of moisture. Thus, the Curie temperature is expected to be much higher than the decomposition temperature in this case.

The magnitude of polarization was computed to be 3.18 and 3.42 $\mu C/cm^2$ using both the Berry phase and the Born effective charge methods, respectively, as shown in Figure 5c and Table 1. To ensure that the polarization computations are correct, multiple structures along the pathway connecting the up- and the down-polarization state were constructed such that a hypothetical centrosymmetric structure (with a point group symmetry of $2/m$) are also included. More comments on the relevance of this hypothetical centrosymmetric structure will be made later. For the Born effective charge calculation, this hypothetical centrosymmetric structure was used as the reference state. As is evident from Figure 5c, the polarization results of both the Berry phase and the Born effective charge calculations lie on the same polarization lattice and are consistent with each other.

Besides having a nonzero polarization, the energy barriers to reverse the polarization should also be low for a material to be ferroelectric. Thus, we explored two pathways to switch the polarization between two opposite states. While one is guided by group-theoretical considerations (through predicted parent $Immm$ phase), the other is based on a direct pathway connecting the two opposite polar states (through $P2/c$ phase). The results for the low energy barriers of 52 and 38.54 meV/atom obtained using the NEB method are shown in Figure 5d. Both pathways can be expected to be active during the polarization-switching process as the energy barriers in both cases are small and comparable. The energy barrier and polarization reversal plots can also be combined together, and polarization−electric field curves can be approached based on differentiation of free energy with respect to polarization. For the case of CaO_2, these curves are included in the SI.

https://dx.doi.org/10.1021/acs.chemmater.9b05324
Chem. Mater. 2020, 32, 3823−3832

Table 2. Comparison between the Structural Parameters of the $Pna2_1$ Phase of CaO_2 Obtained from XRD Experiments and DFT Computations (in brackets)

$Pna2_1$	a	b	c
(33)	7.102843 (7.12880)	3.593601 (3.62719)	5.925604 (5.96123)
atom	x	y	z
Ca (4a)	0.123 (0.1259)	0.16 (0.1531)	0.00574 (−0.00091)
O (4a)	−0.166 (−0.16707)	−0.158 (−0.15734)	−0.0875 (−0.09457)
O (4a)	−0.412 (−0.41915)	0.174 (0.14988)	−0.386 (−0.39472)

On the basis of the favorable predictions on the stability, the nonzero magnitude of polarization, and the presence of low-energy pathways for polarization reversal, one can expect CaO_2 to be a potential ferroelectric oxide (at least in the temperature−pressure range where polar $Pna2_1$ phase is stable in Figure 5) . Indisputable proof of FE behavior in CaO_2 would require the fabrication of samples suitable for dielectric property measurements (thin films, crystals, or dense polycrystalline bodies) for which several challenges are encountered owing to its stability at elevated temperatures coupled with its propensity to easily react, as discussed in detail in the SI (section B). Nonetheless, pure CaO_2 powders do crystallize in the polar $Pna2_1$ phase, as confirmed by the XRD results shown in Figure 6. Details on the synthesis of CaO_2 powders and their subsequent characterization using XRD measurements are given in the SI (section A). These measurements confirmed the stability of the polar $Pna2_1$ phase over the temperature range from −100 to 300 °C. Above ∼300 °C, this polar phase was found to be unstable, perhaps due to its decomposition into $Ca(OH)_2$ (see more details in Figures S1 and S2 in the SI). A comparison between the structural parameters as obtained using the diffraction studies and the DFT computations is also provided in Table 2. An excellent agreement is evident.

As another example besides CaO_2, we computed the phase diagram, spontaneous polarization, and energy barriers for polarization reversal in the case of SrO_2 (see Figure S4 and section F in the SI). However, among the two peroxides, CaO_2 was found to be more interesting, as SrO_2 had a spontaneous polarization of just ∼1.7 $\mu C/cm^2$. Further, while there was a clear stability window for the polar phase in the case of CaO_2, there were many energetically similar (within 1 meV/atom) nonpolar phases for SrO_2, making it difficult to unambiguously determine the equilibrium phase in this case.

Finally, we note that while on one hand identification of many potential FE candidates oxides with low-energy polar polymorphs, similar to the case of hafnia, strongly advocates the possibility of discovery or engineering ferroelectricity in other oxides/binaries, on the other hand, difficulties encountered in the synthesis of dense films or monolithic (poly)-crystalline bodies for conclusive FE measurements highlight the challenges that remain to be overcome, as well as the considerations absent from our computational strategy. An equally important outcome of this work is the general computational strategy, combining structural search, first-principles density functional theory, and group-theoretical methods, to search for functional (FE, pyroelectric, or polar) materials of any class.

CONCLUSIONS

In conclusion, learning from the recent discovery of ferroelectricity in hafnia, a computational strategy was employed to search for potential ferroelectric behavior within the class of materials comprising the binary oxides, otherwise known for their linear dielectric properties. The strategy involved several steps, including (1) identification of low-energy phases of a material (performed using minima-hopping algorithm), (2) classification of identified phases into polar and nonpolar structures, (3) determination of plausible parent phase for interesting low-energy polar phases using group-theoretical considerations, and (4) finally, computation of spontaneous polarization (using Berry phase) and minimum energy pathways for polarization switching (using NEB).

Out of the 21 simple binary oxides studied using this strategy, 15 were found to exhibit low-energy metastable polar phases, with BeO and ZnO displaying a polar ground state and CaO_2 and SrO_2 having a polar phase extremely close in energy to the ground state (within DFT noise). To find conditions in which the polar phase maybe favored, the phase stability of 15 promising candidates—with stable/metastable polar phases—was studied under various pressures. While in the case of ZrO_2, HfO_2, Ga_2O_3, Sc_2O_3, Al_2O_3, TiO_2, and BaO_2 the metastable polar phases were found to come very close in energy (<20 meV/atom) to the equilibrium phases, conditions stabilizing the polar $Pna2_1$ (SG 33) phase in CaO_2 and SrO_2, the polar $P6_3mc$ (SG 186) phase in BeO and ZnO, and the polar $Cmc2_1$ phase in B_2O_3 as the ground state were identified. Next, polarization reversal energy barriers were computed for 11 oxides found to have polar phase with an energy within 20 meV/atom to the ground state over a pressure range of 0−30 GPa, revealing 5 new simple oxides as potential FE candidates—CaO_2 ($Pna2_1$, 33), SrO_2 ($Pna2_1$, 33), Ga_2O_3 ($Pna2_1$, 33), Al_2O_3 ($Pna2_1$, 33), and TiO_2 ($Pca2_1$, 29)—while 2 oxides already known for their potential FE properties (HfO_2 and ZrO_2) were recovered to have low-energy metastable polar phases. In addition, B_2O_3 ($Cmc2_1$, 36) and Sc_2O_3 ($Cmc2_1$, 36) were identified as potential pyroelectric candidates owing to large polarization reversal barriers, with BeO ($P6_3mc$, 186) and ZnO ($P6_3mc$, 186) also correctly recovered as pyroelectric oxides.

CaO_2 was further studied in detail. The computations identified $Immm$ (SG 71) as the likely space group of the parent phase, revealed a spontaneous polarization in the ferroelectric phase of 3.18 $\mu C/cm^2$, and demonstrated a polarization reversal pathway with a minimum energy barrier of 38.54 meV/atom. Synchrotron XRD measurements confirmed that CaO_2 crystallizes in the polar $Pna2_1$ phase, in agreement with theory, suggesting potential as a ferroelectric oxide. However, there are challenges that must be overcome to prepare monolithic specimens suitable for the polarization-switching measurements.

On the basis of the high occurrence of low-energy stable and metastable polar phases in binary oxides, our work highlights that many more simple oxides and other binaries—beyond hafnia and traditional perovskite materials—could display ferroelectric behavior. Thus, further studies identifying

https://dx.doi.org/10.1021/acs.chemmater.9b05324
Chem. Mater. 2020, 32, 3823−3832

conditions stabilizing the low-energy polar phases in more promising oxides, such as Ga_2O_3, Al_2O_3, and TiO_2, could also reveal hidden ferroelectric functionalities of these oxides. Previous diffraction data hinting at the formation of polar phases in the case of Al_2O_3 and Ga_2O_3 further supports the conclusions made in this work and highlights the need for careful (re)analysis of diffraction data for all of the identified interesting candidate oxides to find clues for the formation of polar phases in such cases. Overall, this work has revealed the opportunities and provided a strategy for systematically searching and discovering ferroelectricity and other functional materials.

■ ASSOCIATED CONTENT

Supporting Information

The Supporting Information is available free of charge at https://pubs.acs.org/doi/10.1021/acs.chemmater.9b05324.

Discussion on the synthesis and characterization of CaO_2 samples, challenges encountered in their dielectric measurements, free energy trends for different phases of CaO_2 and SrO_2, effect of pressure on the phase stability of promising oxides and the phonon band structure of different polar phases, energy vs polarization and derived polarization vs electric field behavior, and polarization reversal energy barrier using DFT NEB calculations (PDF)

■ AUTHOR INFORMATION

Corresponding Author

Rampi Ramprasad − *School of Materials Science and Engineering, Georgia Institute of Technology, Atlanta, Georgia 30332, United States;* orcid.org/0000-0003-4630-1565; Email: rampi.ramprasad@mse.gatech.edu

Authors

Rohit Batra − *School of Materials Science and Engineering, Georgia Institute of Technology, Atlanta, Georgia 30332, United States;* orcid.org/0000-0002-1098-7035

Huan Doan Tran − *School of Materials Science and Engineering, Georgia Institute of Technology, Atlanta, Georgia 30332, United States;* orcid.org/0000-0002-8093-9426

Brienne Johnson − *Department of Materials Science and Engineering, North Carolina State University, Raleigh, North Carolina 27607, United States*

Brandon Zoellner − *Department of Chemistry, North Carolina State University, Raleigh, North Carolina 27695, United States*

Paul A. Maggard − *Department of Chemistry, North Carolina State University, Raleigh, North Carolina 27695, United States*

Jacob L. Jones − *Department of Materials Science and Engineering, North Carolina State University, Raleigh, North Carolina 27607, United States*

George A. Rossetti, Jr. − *Department of Materials Science and Engineering, University of Connecticut, Storrs, Connecticut 06269, United States*

Complete contact information is available at: https://pubs.acs.org/10.1021/acs.chemmater.9b05324

Author Contributions

‡R.B. and H.D.T.: These authors contributed equally to this work.

Notes

The authors declare no competing financial interest.

■ ACKNOWLEDGMENTS

Financial support of this work through Grant No. W911NF-15-1-0593 from the Army Research Office (ARO) and partial computational support through an Extreme Science and Engineering Discovery Environment (XSEDE) allocation number TG-DMR080058N are acknowledged. This research used resources of the Advanced Photon Source, a U.S. Department of Energy (DOE) Office of Science User Facility operated for the DOE Office of Science by Argonne National Laboratory under Contract No. DE-AC02-06CH11357. This work was performed in part at the Analytical Instrumentation Facility (AIF) at North Carolina State University, which is supported by the State of North Carolina and the National Science Foundation (award number ECCS-1542015). The AIF is a member of the North Carolina Research Triangle Nanotechnology Network (RTNN), a site in the National Nanotechnology Coordinated Infrastructure (NNCI).

■ REFERENCES

(1) Böscke, T. S.; Müller, J.; Bräuhaus, D.; Schröder, U.; Böttger, U. Ferroelectricity in hafnium oxide thin films. *Appl. Phys. Lett.* **2011**, *99*, 102903.

(2) Böscke, T. S.; Teichert, S.; Bräuhaus, D.; Müller, J.; Schröder, U.; Böttger, U.; Mikolajick, T. Phase transitions in ferroelectric silicon doped hafnium oxide. *Appl. Phys. Lett.* **2011**, *99*, 112904.

(3) Mueller, S.; Mueller, J.; Singh, A.; Riedel, S.; Sundqvist, J.; Schroeder, U.; Mikolajick, T. Incipient ferroelectricity in Al-doped HfO2 thin films. *Adv. Funct. Mater.* **2012**, *22*, 2412−2417.

(4) Müller, J.; Böscke, T. S.; Schröder, U.; Mueller, S.; Bräuhaus, D.; Böttger, U.; Frey, L.; Mikolajick, T. Ferroelectricity in simple binary ZrO2 and HfO2. *Nano Lett.* **2012**, *12*, 4318−4323.

(5) Schroeder, U., Hwang, C. S., Funakubo, H., Eds. *Ferroelectricity in Doped Hafnium Oxide: Materials, Properties and Devices*; Woodhead Publishing, 2019.

(6) Materlik, R.; Künneth, C.; Kersch, A. The origin of ferroelectricity in Hf1-x Zrx O2: A computational investigation and a surface energy model. *J. Appl. Phys.* **2015**, *117*, 134109.

(7) Batra, R.; Tran, H. D.; Ramprasad, R. Stabilization of metastable phases in hafnia owing to surface energy effects. *Appl. Phys. Lett.* **2016**, *108*, 172902.

(8) Batra, R.; Huan, T. D.; Jones, J. L.; Rossetti, G.; Ramprasad, R. Factors favoring ferroelectricity in hafnia: A first-principles computational study. *J. Phys. Chem. C* **2017**, *121*, 4139−4145.

(9) Batra, R.; Huan, T. D.; Rossetti, G. A.; Ramprasad, R. Dopants Promoting Ferroelectricity in Hafnia: Insights from a comprehensive Chemical Space Exploration. *Chem. Mater.* **2017**, *29*, 9102−9109.

(10) Reyes-Lillo, S. E.; Garrity, K. F.; Rabe, K. M. Antiferroelectricity in thin-film ZrO_2 from first principles. *Phys. Rev. B: Condens. Matter Mater. Phys.* **2014**, *90*, 140103.

(11) Park, M. H.; Lee, Y. H.; Kim, H. J.; Kim, Y. J.; Moon, T.; Kim, K. D.; Hyun, S. D.; Mikolajick, T.; Schroeder, U.; Hwang, C. S. Understanding the formation of the metastable ferroelectric phase in hafnia−zirconia solid solution thin films. *Nanoscale* **2018**, *10*, 716−725.

(12) Robertson, J. High dielectric constant gate oxides for metal oxide Si transistors. *Rep. Prog. Phys.* **2006**, *69*, 327−396.

(13) Zhu, H.; Tang, C.; Fonseca, L. R. C.; Ramprasad, R. Recent progress in ab initio simulations of hafnia-based gate stacks. *J. Mater. Sci.* **2012**, *47*, 7399−7416.

(14) Ramprasad, R.; Shi, N. Dielectric properties of nanoscale HfO2 slabs. *Phys. Rev. B: Condens. Matter Mater. Phys.* **2005**, *72*, 052107.

(15) Huan, T. D.; Sharma, V.; Rossetti, G. A.; Ramprasad, R. Pathways towards ferroelectricity in hafnia. *Phys. Rev. B: Condens. Matter Mater. Phys.* **2014**, *90*, 064111.

(16) Bousquet, E.; Spaldin, N. A.; Ghosez, P. Strain-Induced ferroelectricity in simple rocksalt binary oxides. *Phys. Rev. Lett.* **2010**, *104*, 037601.

(17) Bennett, J. W.; Garrity, K. F.; Rabe, K. M.; Vanderbilt, D. Hexagonal *ABC* semiconductors as ferroelectrics. *Phys. Rev. Lett.* **2012**, *109*, 167602.
(18) Bennett, J. W.; Grinberg, I.; Davies, P. K.; Rappe, A. M. Pb-free ferroelectrics investigated with density functional theory: $SnAl_{1/2}Nb_{1/2}O_3$ perovskites. *Phys. Rev. B: Condens. Matter Mater. Phys.* **2011**, *83*, 144112.
(19) Bennett, J. W.; Rabe, K. M. Integration of first-principles methods and crystallographic database searches for new ferroelectrics: Strategies and explorations. *J. Solid State Chem.* **2012**, *195*, 21−31.
(20) Garrity, K. F. High-throughput first-principles search for new ferroelectrics. *Phys. Rev. B: Condens. Matter Mater. Phys.* **2018**, *97*, 024115.
(21) Abrahams, S. C. Systematic prediction of new ferroelectrics in space group R3. II. *Acta Crystallogr., Sect. B: Struct. Sci.* **2007**, *63*, 257−269.
(22) Hohenberg, P.; Kohn, W. Inhomogeneous electron gas. *Phys. Rev.* **1964**, *136* (3B), B864−B871.
(23) Kohn, W.; Sham, L. J. Self-consistent equations including exchange and correlation effects. *Phys. Rev.* **1965**, *140*, A1133−A1138.
(24) Kresse, G.; Furthmüller, J. Efficient iterative schemes for ab initio total-energy calculations using a plane-wave basis set. *Phys. Rev. B: Condens. Matter Mater. Phys.* **1996**, *54*, 11169.
(25) Perdew, J. P.; Burke, K.; Ernzerhof, M. Generalized gradient approximation made simple. *Phys. Rev. Lett.* **1996**, *77*, 3865−3868.
(26) Huan, T. D.; Mannodi-Kanakkithodi, A.; Kim, C.; Sharma, V.; Pilania, G.; Ramprasad, R. A polymer dataset for accelerated property prediction and design. *Sci. Data* **2016**, *3*, 160012.
(27) Pack, J. D.; Monkhorst, H. J. Special points for Brillouin-zone integrations"-a reply. *Phys. Rev. B* **1977**, *16*, 1748−1749.
(28) Oganov, A. R. *Modern Methods of Crystal Structure Prediction*; Wiley-VCH: Weinheim, Germany, 2011.
(29) Goedecker, S. Minima hopping: An efficient search method for the global minimum of the potential energy surface of complex molecular systems. *J. Chem. Phys.* **2004**, *120*, 9911−9917.
(30) Amsler, M.; Goedecker, S. Crystal structure prediction using the minima hopping method. *J. Chem. Phys.* **2010**, *133*, 224104.
(31) Tran, H. D.; Amsler, M.; Botti, S.; Marques, M. A.; Goedecker, S. First-principles predicted low-energy structures of NaSc(BH4)4. *J. Chem. Phys.* **2014**, *140*, 124708.
(32) Huan, T. D.; Amsler, M.; Tuoc, V. N.; Willand, A.; Goedecker, S. Low-energy structures of zinc borohydride Zn(BH4)2. *Phys. Rev. B: Condens. Matter Mater. Phys.* **2012**, *86*, 224110.
(33) Baldwin, A. F.; Huan, T. D.; Ma, R.; Mannodi-Kanakkithodi, A.; Tefferi, M.; Katz, N.; Cao, Y.; Ramprasad, R.; Sotzing, G. A. Rational design of organotin polyesters. *Macromolecules* **2015**, *48*, 2422−2428.
(34) Togo, A.; Oba, F.; Tanaka, I. First-principles calculations of the ferroelastic transition between rutile-type and CaCl 2-type SiO 2 at high pressures. *Phys. Rev. B: Condens. Matter Mater. Phys.* **2008**, *78*, 134106.
(35) Stokes, H. T.; Hatch, D. M. FINDSYM: program for identifying the space-group symmetry of a crystal. *J. Appl. Crystallogr.* **2005**, *38*, 237−238.
(36) Nelson, J. R.; Needs, R. J.; Pickard, C. J. Calcium peroxide from ambient to high pressures. *Phys. Chem. Chem. Phys.* **2015**, *17*, 6889−6895.
(37) Königstein, M.; Catlow, C. R. A. Ab initioquantum mechanical study of the structure and stability of the alkaline earth metal oxides and peroxides. *J. Solid State Chem.* **1998**, *140*, 103−115.
(38) Shuvalov, L. A. Symmetry aspects of ferroelectricity. *J. Phys. Soc. Jpn. (Supp)* **1970**, *28*, 38−51.
(39) King-Smith, R. D.; Vanderbilt, D. Theory of polarization of crystalline solids. *Phys. Rev. B: Condens. Matter Mater. Phys.* **1993**, *47*, 1651−1654.
(40) Resta, R. Macroscopic polarization in crystalline dielectrics: The geometric phase approach. *Rev. Mod. Phys.* **1994**, *66*, 899−915.
(41) Sheppard, D.; Xiao, P.; Chemelewski, W.; Johnson, D. D.; Henkelman, G. A generalized solid-state nudged elastic band method. *J. Chem. Phys.* **2012**, *136*, 074103.
(42) Gonze, X.; Lee, C. Dynamical matrices, Born effective charges, dielectric permittivity tensors, and interatomic force constants from density-functional perturbation theory. *Phys. Rev. B: Condens. Matter Mater. Phys.* **1997**, *55*, 10355.
(43) Huan, T. D.; Tuoc, V. N.; Minh, N. V. Layered structures of organic/inorganic hybrid halide perovskites. *Phys. Rev. B: Condens. Matter Mater. Phys.* **2016**, *93*, 094105.
(44) Reyes-Lillo, S. E.; Garrity, K. F.; Rabe, K. M. Antiferroelectricity in thin-film ZrO 2 from first principles. *Phys. Rev. B: Condens. Matter Mater. Phys.* **2014**, *90*, 140103.
(45) Posternak, M.; Baldereschi, A.; Catellani, A.; Resta, R. Ab initio study of the spontaneous polarization of pyroelectric BeO. *Phys. Rev. Lett.* **1990**, *64*, 1777.
(46) Liu, J.; Pantelides, S. T. Mechanisms of pyroelectricity in three- and two-dimensional materials. *Phys. Rev. Lett.* **2018**, *120*, 207602.
(47) Garrity, K. F. High-throughput first-principles search for new ferroelectrics. *Phys. Rev. B: Condens. Matter Mater. Phys.* **2018**, *97*, 024115.
(48) Duan, W.; Wentzcovitch, R. M.; Thomson, K. T. First-principles study of high-pressure alumina polymorphs. *Phys. Rev. B: Condens. Matter Mater. Phys.* **1998**, *57*, 10363.
(49) Li, D.; Ching, W. Electronic structures and optical properties of low-and high-pressure phases of crystalline B 2 O 3. *Phys. Rev. B: Condens. Matter Mater. Phys.* **1996**, *54*, 13616.
(50) Huang, L.; Durandurdu, M.; Kieffer, J. New B2O3 crystals predicted from concurrent molecular dynamics simulations and first-principles calculations. *J. Phys. Chem. C* **2007**, *111*, 13712−13720.
(51) Yoshioka, S.; Hayashi, H.; Kuwabara, A.; Oba, F.; Matsunaga, K.; Tanaka, I. Structures and energetics of Ga2O3 polymorphs. *J. Phys.: Condens. Matter* **2007**, *19*, 346211.
(52) Canepa, P.; Ugliengo, P.; Alfredsson, M. Elastic and vibrational properties of α-and β-PbO. *J. Phys. Chem. C* **2012**, *116*, 21514−21522.
(53) Levin, I.; Brandon, D. Metastable alumina polymorphs: crystal structures and transition sequences. *J. Am. Ceram. Soc.* **1998**, *81*, 1995−2012.
(54) Gross, H.-L.; Mader, W. On the crystal structure of κ-alumina. *Chem. Commun.* **1997**, 55−56.
(55) Zhou, X.-F.; Dong, X.; Qian, G.-R.; Zhang, L.; Tian, Y.; Wang, H.-T.; et al. Unusual compression behavior of TiO2 polymorphs from first principles. *Phys. Rev. B: Condens. Matter Mater. Phys.* **2010**, *82*, 060102.
(56) Abbasnejad, M.; Mohammadizadeh, M.; Maezono, R. Structural, electronic, and dynamical properties of Pca21-TiO2 by first principles. *EPL-Europhys. Lett.* **2012**, *97*, 56003.
(57) Zhao, X.; Nguyen, M. C.; Wang, C.-Z.; Ho, K.-M. Structures and stabilities of alkaline earth metal peroxides XO 2 (X= Ca, Be, Mg) studied by a genetic algorithm. *RSC Adv.* **2013**, *3*, 22135−22139.
(58) Zhang, Y.; Sun, J.; Perdew, J. P.; Wu, X. Comparative first-principles studies of prototypical ferroelectric materials by LDA, GGA, and SCAN meta-GGA. *Phys. Rev. B: Condens. Matter Mater. Phys.* **2017**, *96*, 035143.
(59) Sawada, S.; Hirotsu, S.; Iwamura, H.; Shiroishi, Y. A Ferroelectric Type of Hysteresis Loop Observed in BeO. *J. Phys. Soc. Jpn.* **1973**, *35*, 946−946.
(60) Moriwake, H.; Konishi, A.; Ogawa, T.; Fujimura, K.; Fisher, C. A.; Kuwabara, A.; Shimizu, T.; Yasui, S.; Itoh, M. Ferroelectricity in wurtzite structure simple chalcogenide. *Appl. Phys. Lett.* **2014**, *104*, 242909.
(61) Beckman, S.; Wang, X.; Rabe, K. M.; Vanderbilt, D. Ideal barriers to polarization reversal and domain-wall motion in strained ferroelectric thin films. *Phys. Rev. B: Condens. Matter Mater. Phys.* **2009**, *79*, 144124.